

Quantum Fluctuations of a Coulomb Potential as a Source of Flicker Noise

Kirill A. Kazakov*

*Department of Theoretical Physics, Physics Faculty,
Moscow State University, 119899, Moscow, Russian Federation*

The power spectrum of quantum fluctuations of the electromagnetic field produced by an elementary particle is determined. It is found that in a wide range of practically important frequencies the power spectrum of fluctuations exhibits an inverse frequency dependence. The magnitude of fluctuations produced by a conducting sample is shown to have a Gaussian distribution around its mean value, and its dependence on the sample geometry is determined. In particular, it is demonstrated that for geometrically similar samples the power spectrum is inversely proportional to the sample volume. It is argued also that the magnitude of fluctuations induced by external electric field is proportional to the field strength squared. A comparison with experimental data on flicker noise measurements in continuous metal films is made.

PACS numbers: 12.20.-m, 42.50.Lc

Keywords: Quantum fluctuations, electromagnetic field, flicker noise, correlation function, long-range expansion

I. INTRODUCTION

Measurements of voltage fluctuations in various media show that at sufficiently low frequencies, power spectra of fluctuations in all conducting materials exhibit a universal profile which is close to inverse frequency dependence, and called for this reason a flicker $1/f$ -noise. Although this noise is dominating only at low frequencies, experiments show the presence of the $1/f$ -component in the whole measured band, from $10^{-6}Hz$ to 10^6Hz . Also, the following three main characteristic properties are universally held: The $1/f$ -noise produced by a conducting sample 1) is inversely proportional to its volume, 2) is Gaussian, and 3) its part induced by external electric field is proportional to the field strength squared.

A number of mechanisms has been put forward to explain the origin of the $1/f$ -noise. The property 3) is typical for resistive systems, and suggests that the flicker noise can arise from resistance fluctuations [1]. It has been also proposed that fluctuations in the carrier mobility [2, 3], or in the number of carriers caused by surface traps [4] might explain the origin of the $1/f$ -profile of the power spectrum. All these models, however, have restricted validity, because they involve one or another assumption specific to the problem under consideration. For instance, assuming that the resistance fluctuations in the first of the above-mentioned models spring from temperature fluctuations, one has to choose an appropriate spatial correlation of these fluctuations in order to obtain the $1/f$ -profile of the power spectrum [5]. Similarly, the model suggested in Ref. [4] requires a specific distribution of trapping times, etc. In addition to that, the models suggested so far reproduce the $1/f$ -profile only in a restricted range of frequencies. On the other hand, the ubiquity of the flicker noise, and universality of its properties imply that there must exist a simple and universal, and therefore, fundamental underlying reason. It is natural to look for this reason in the quantum properties of charge carriers. In this direction, the problem has been extensively investigated by Handel and co-workers [6]. Handel's approach is based on the theory of infrared radiative corrections in quantum electrodynamics. Handel showed that the $1/f$ power spectrum of photons emitted in any scattering process can be derived from the well-known property of bremsstrahlung, namely, from the infrared divergence of the cross-section considered as a function of the energy loss. Thus, this theory treats the $1/f$ -noise as a relativistic effect (in fact, the noise level in this theory $\sim \alpha(\Delta v)^2/c^2$, where α is the fine structure constant, Δv velocity change of the particle being scattered, and c the speed of light). It should be mentioned, however, that the Handel's theory has been severely criticized in many respects [7, 8].

The purpose of this paper is to draw attention to another quantum aspect of the electromagnetic interaction, which is of a purely nonrelativistic nature. It turns out that there is a simple and quite general property of the electromagnetic interactions of quantized matter, which may be the origin of flicker noise. Namely, it will be shown below that the power spectrum of the Coulomb field fluctuations produced by spreading wave packet of a free charged particle exhibits an inverse frequency dependence in the low-frequency limit. We will show also that the power spectrum possesses the three above-mentioned characteristic properties of flicker noise as well.

*Electronic address: kirill@phys.msu.ru

The main tool we use in investigating quantum fluctuations of the Coulomb field produced by a quantum particle is the two-point correlation function of the electromagnetic field. Properties of this function in the coincidence limit were investigated in detail in Ref. [9]. It was found, in particular, that the root mean square fluctuation of the Coulomb potential is of zeroth order in the Planck constant \hbar . It was shown, furthermore, that the Fourier transform of the correlation function with respect to time exhibits an inverse frequency dependence in the low-frequency limit. One of the goals of the present paper is to show that essentially the same formula describes also the low-frequency limit of the power spectrum of fluctuating electromagnetic fields measured at *two distinct* time instants. The reason underlying this similarity is that in both cases the leading contribution to the correlation function is contained in its disconnected part.

The paper is organized as follows. In Sec. II a preliminary consideration of the problem is given, and the Schwinger-Keldysh formalism used throughout the work is briefly reviewed. The low-frequency asymptotic of the power spectrum is calculated in Sec. III. It is proved in Sec. III A that the low-frequency asymptotic of the connected part of the correlation function is logarithmic. Contribution of the disconnected part is calculated exactly in Sec. III B, and is shown to exhibit an inverse frequency dependence. The obtained result is analyzed to verify that it is in agreement with the above-mentioned general characteristics of flicker noise, and then compared with experimental data in Sec. III C. Section IV summarizes the results of the work and states the conclusion.

II. PRELIMINARIES

Let us consider a single particle with mass m and electric charge e . In classical theory, the electromagnetic field produced by such particle at rest is described by the Coulomb potential

$$A_0 = \frac{e}{4\pi r}, \quad \mathbf{A} = 0. \quad (1)$$

Our aim is to determine quantum properties of this potential. More precisely, we will be concerned with the quantum fluctuations of the field-theoretic counterpart of this potential at the zeroth order in the Planck constant \hbar .

In quantum theory, Eq. (1) is reproduced by calculating the corresponding mean fields, $\langle \text{in} | \hat{A}_0 | \text{in} \rangle$, $\langle \text{in} | \hat{\mathbf{A}} | \text{in} \rangle$. In the Schwinger-Keldysh formalism [10, 11], they are given by

$$\langle \text{in} | \hat{A}^\mu | \text{in} \rangle = \int \mathcal{D}\Phi_- \int \mathcal{D}\Phi_+ A_+^\mu \exp\{iS[\Phi_+] - iS[\Phi_-]\}, \quad (2)$$

where the subscript $+$ ($-$) shows that the time argument of the integration variable runs from $-\infty$ to $+\infty$ (from $+\infty$ to $-\infty$). Integration is over all fields satisfying

$$\begin{aligned} A_\pm^+ \rightarrow 0, \quad \phi_\pm^+ \rightarrow \phi_0^+, \quad (\phi^*)_\pm^+ \rightarrow (\phi_0^*)^+ \quad & \text{for } t \rightarrow -\infty, \\ \Phi_+ = \Phi_- \quad & \text{for } t \rightarrow +\infty, \end{aligned} \quad (3)$$

where Φ collectively denotes the fundamental fields of the theory, $\Phi = \{A_\mu, \phi, \phi^*\}$, the components ϕ, ϕ^* describing the charged particle which for simplicity will be assumed scalar, ϕ_0 is the given particle state, $\mathcal{D}\Phi$ the invariant integral measure, and $S = S[\Phi]$ the action functional of the system. Assuming that the gradient invariance of the theory is fixed by the Lorentz condition

$$G \equiv \partial^\mu A_\mu = 0, \quad (4)$$

the action takes the form

$$\begin{aligned} S[\Phi] &= S_0[\Phi] + S_{\text{gf}}[\Phi], \\ S_0[\Phi] &= \int d^4x \{(\partial_\mu \phi^* + ieA_\mu \phi^*)(\partial^\mu \phi - ieA^\mu \phi) - m^2 \phi^* \phi\} - \frac{1}{4} \int d^4x F_{\mu\nu} F^{\mu\nu}, \\ S_{\text{gf}}[\Phi] &= -\frac{1}{2} \int d^4x G^2, \quad F_{\mu\nu} = \partial_\mu A_\nu - \partial_\nu A_\mu. \end{aligned} \quad (5)$$

Diagrammatics generated upon expanding the integral (2) in powers of the coupling constant e consists of the following elements. There are four types of pairings for each field A_μ or ϕ , corresponding to the four different ways of placing

two field operators on the two branches of the time path. They are conveniently combined into 2×2 matrices¹

$$\mathfrak{D}^{\mu\nu}(x, y) = \begin{pmatrix} D_{++}^{\mu\nu}(x, y) & D_{+-}^{\mu\nu}(x, y) \\ D_{-+}^{\mu\nu}(x, y) & D_{--}^{\mu\nu}(x, y) \end{pmatrix} = \begin{pmatrix} i\langle T\hat{A}^\mu(x)\hat{A}^\nu(y)\rangle_0 & i\langle \hat{A}^\nu(y)\hat{A}^\mu(x)\rangle_0 \\ i\langle \hat{A}^\mu(x)\hat{A}^\nu(y)\rangle_0 & i\langle \tilde{T}\hat{A}^\mu(x)\hat{A}^\nu(y)\rangle_0 \end{pmatrix},$$

$$\mathfrak{D}(x, y) = \begin{pmatrix} D_{++}(x, y) & D_{+-}(x, y) \\ D_{-+}(x, y) & D_{--}(x, y) \end{pmatrix} = \begin{pmatrix} i\langle T\hat{\phi}(x)\hat{\phi}^\dagger(y)\rangle_0 & i\langle \hat{\phi}^\dagger(y)\hat{\phi}(x)\rangle_0 \\ i\langle \hat{\phi}(x)\hat{\phi}^\dagger(y)\rangle_0 & i\langle \tilde{T}\hat{\phi}(x)\hat{\phi}^\dagger(y)\rangle_0 \end{pmatrix},$$

where the operation of time ordering T (\tilde{T}) arranges the factors so that the time arguments decrease (increase) from left to right, and $\langle \cdot \rangle_0$ denotes vacuum averaging. The “propagators” $\mathfrak{D}_{\mu\nu}$, \mathfrak{D} satisfy the following matrix equations

$$\int d^4z \mathfrak{G}_{\mu\nu}(x, z)\mathfrak{D}^{\nu\alpha}(z, y) = -\epsilon^\alpha_\mu \delta^{(4)}(x - y), \quad \mathfrak{G}_{\mu\nu}(x, y) = i \frac{\delta^2 S^{(2)}}{\delta A^\mu(x) \delta A^\nu(y)}, \quad (6)$$

$$\int d^4z \mathfrak{G}(x, z)\mathfrak{D}(z, y) = -\epsilon \delta^{(4)}(x - y), \quad \mathfrak{G}(x, y) = i \frac{\delta^2 S^{(2)}}{\delta \phi^*(x) \delta \phi(y)}, \quad (7)$$

where $S^{(2)}$ is the free field part of the action, ϵ , i are 2×2 matrices with respect to indices $+$, $-$:

$$\epsilon = \begin{pmatrix} 1 & 0 \\ 0 & 1 \end{pmatrix}, \quad i = \begin{pmatrix} 1 & 0 \\ 0 & -1 \end{pmatrix}.$$

As in the ordinary Feynman diagrammatics of the S-matrix theory, the propagators are contracted with the vertex factors generated by the interaction part of the action, $S^{\text{int}}[\Phi] = S[\Phi] - S^{(2)}[\Phi]$, with subsequent summation over $(+, -)$ in the vertices, each “ $-$ ” vertex coming with an extra factor (-1) . This can be represented as the matrix multiplication of $\mathfrak{D}_{\mu\nu}$, \mathfrak{D} with suitable matrix vertices. For instance, the $A\partial\phi\phi^*$ part of the action generates the matrix vertex \mathfrak{V} which in components has the form

$$V_{ijk}^\mu(x, y, z) = s_{ijk} \left. \frac{\delta^3 S}{\delta A_\mu(x) \delta \phi(y) \delta \phi^*(z)} \right|_{\Phi=0},$$

where the indices i, j, k take the values $+, -$, and s_{ijk} is defined by $s_{+++} = -s_{---} = 1$ and zero otherwise. External ϕ (ϕ^*) line is represented in this notation by a column (row)

$$\mathfrak{r} = \begin{pmatrix} \phi_0 \\ \phi_0^* \end{pmatrix}, \quad \mathfrak{r}^\dagger = (\phi_0^*, \phi_0^*),$$

satisfying

$$\int d^4z \mathfrak{G}(x, z)\mathfrak{r}(z) = \begin{pmatrix} 0 \\ 0 \end{pmatrix}, \quad \int d^4x \mathfrak{r}^\dagger(x)\mathfrak{G}(x, z) = (0, 0). \quad (8)$$

The tree diagrams contributing to the right hand side of Eq. (2) are depicted in Fig. 1. Of these only the diagram in Fig. 1(a) gives rise to a non-zero contribution. The momentum flow in the other diagram is inconsistent with the momentum conservation in the vertex for any non-zero value of the momentum transfer p_μ , because the lines of this diagram are all on the mass shell. The same diagram 1(a) represents also the tree value of the in-out matrix element $\langle \text{out} | \hat{A}^\mu(x) | \text{in} \rangle$ calculated using the ordinary Feynman rules. This is natural because we are concerned here with a one-point function whose matrix element is evaluated between one-particle states for which $|\text{in}\rangle$ is essentially the same as $|\text{out}\rangle$. The things change, however, if we want to determine the field fluctuation. In the Schwinger-Keldysh formalism, the expectation value of the product $\hat{A}^\mu(x)\hat{A}^\nu(x')$ has the form

$$\langle \text{in} | \hat{A}^\mu(x)\hat{A}^\nu(x') | \text{in} \rangle = \int \mathcal{D}\Phi_- \int \mathcal{D}\Phi_+ A_-^\mu(x) A_+^\nu(x') \exp\{iS[\Phi_+] - iS[\Phi_-]\}, \quad (9)$$

¹ Below, Gothic letters are used to distinguish quantities representing columns, matrices etc. with respect to indices $+$, $-$.

The corresponding tree diagrams are shown in Fig. 2. We see that these diagrams *differ* from those we would have obtained applying the ordinary Feynman rules to the quantity $\langle \text{out} | \hat{A}^\mu(x) \hat{A}^\nu(x') | \text{in} \rangle$. We define the correlation function of the electromagnetic field fluctuations by

$$C_{\mu\nu}(x, x') = \langle \text{in} | \hat{A}_\mu(x) \hat{A}_\nu(x') | \text{in} \rangle - \langle \text{in} | \hat{A}_\mu(x) | \text{in} \rangle \langle \text{in} | \hat{A}_\nu(x') | \text{in} \rangle. \quad (10)$$

The first term in this definition is usually written in a symmetrical form thus rendering the function $C_{\mu\nu}(x, x')$ real. However, this makes no difference for what follows because it will be shown below that the leading low-frequency term of the correlation function is contained entirely in its disconnected part [the second term in Eq. (10)].

We are concerned with the power spectrum of correlations in the values of the electromagnetic fields measured at two distinct time instants (spatial separation between the observation points, $|\mathbf{x} - \mathbf{x}'|$, is also kept arbitrary). Thus, fixing one of the time arguments, say, t' , we define the Fourier transform of $C_{\mu\nu}(x, x')$ with respect to $(t - t')$

$$C_{\mu\nu}(\mathbf{x}, \mathbf{x}', t', \omega) = \int_{-\infty}^{+\infty} dt C_{\mu\nu}(x, x') e^{i\omega(t-t')}. \quad (11)$$

To complete the present section, we write out explicit expressions for various pairings of the photon and scalar fields

$$\begin{aligned} \mathfrak{D}_{\mu\nu} &= -\eta_{\mu\nu} \mathfrak{D}^0, \quad \mathfrak{D}^0 \equiv \mathfrak{D}|_{m=0}, \\ D_{++}(x, y) &= \int \frac{d^4 k}{(2\pi)^4} \frac{e^{-ik(x-y)}}{m^2 - k^2 - i0}, \quad D_{--}(x, y) = \int \frac{d^4 k}{(2\pi)^4} \frac{e^{-ik(x-y)}}{k^2 - m^2 - i0}, \\ D_{-+}(x, y) &= i \int \frac{d^4 k}{(2\pi)^3} \theta(k^0) \delta(k^2 - m^2) e^{-ik(x-y)}, \quad D_{+-}(x, y) = D_{-+}(y, x). \end{aligned} \quad (12)$$

III. EVALUATION OF THE LEADING CONTRIBUTION

Evaluation of the low-frequency asymptotic of the correlation function proceeds in two steps. First, we will prove in Sec. III A that the low-frequency asymptotic of the connected part of $C_{\mu\nu}$ [the first term in Eq. (10)] is only logarithmic. The contribution of the disconnected part will be calculated exactly in Sec. III B. It will be shown that this contribution exhibits an inverse frequency dependence, and thus dominates in the low-frequency limit.

A. Low-frequency asymptotic of the connected part of correlation function

Before going into detailed calculations, let us first exclude the diagrams in Fig. 2 which do not contain the \hbar^0 contribution. It is not difficult to see that such are the diagrams without internal matter line. Indeed, consider, for instance, the diagram (g). It is proportional to the integral

$$\int d^4 k \theta(k^0) \delta(k^2) \frac{e^{ik(x-x')}}{(k-p)^2},$$

which does not involve the particle mass at all. Taking into account that each external scalar line gives rise to the factor $(2\varepsilon_{\mathbf{q}})^{-1/2}$, where $\varepsilon_{\mathbf{q}} = \sqrt{m^2 + \mathbf{q}^2} \approx m$, we see that the contribution of the diagram 2(g) is proportional to $1/m$. Hence, on dimensional grounds, this diagram is proportional to \hbar . The same is true of all other diagrams without internal matter lines.

The sum of diagrams (a)–(e) in Fig. 2 has the following symbolic form

$$I_{\mu\nu} + I_{\mu\nu}^{\text{tr}}, \quad I_{\mu\nu} = \frac{1}{i} \{ \mathfrak{D}_{\mu\alpha} [\mathfrak{r}^\dagger \mathfrak{V}^\alpha \mathfrak{D} \mathfrak{V}^\beta \mathfrak{r}] \mathfrak{D}_{\beta\nu} \}_{+-},$$

where the superscript “tr” means transposition of the indices and spacetime arguments referring to the points of observation: $\mu \leftrightarrow \nu$, $+\leftrightarrow -$, $x \leftrightarrow x'$ [the transposed contribution is represented by the diagrams collected in part (e)]

of Fig. 2]. Written longhand, $I_{\mu\nu}$ reads

$$I_{\mu\nu}(x, x') = ie^2 \iint d^4z d^4z' \left\{ \begin{aligned} & + D_{++}^0(x, z) \left[\phi_0^*(z) \overset{\leftrightarrow}{\partial}_\mu D_{++}(z, z') \overset{\leftrightarrow}{\partial}'_\nu \phi_0(z') \right] D_{+-}^0(z', x') \\ & - D_{++}^0(x, z) \left[\phi_0^*(z) \overset{\leftrightarrow}{\partial}_\mu D_{+-}(z, z') \overset{\leftrightarrow}{\partial}'_\nu \phi_0(z') \right] D_{--}^0(z', x') \\ & - D_{+-}^0(x, z) \left[\phi_0^*(z) \overset{\leftrightarrow}{\partial}_\mu D_{-+}(z, z') \overset{\leftrightarrow}{\partial}'_\nu \phi_0(z') \right] D_{+-}^0(z', x') \\ & + D_{+-}^0(x, z) \left[\phi_0^*(z) \overset{\leftrightarrow}{\partial}_\mu D_{--}(z, z') \overset{\leftrightarrow}{\partial}'_\nu \phi_0(z') \right] D_{--}^0(z', x') \end{aligned} \right\}, \quad (13)$$

where

$$\varphi \overset{\leftrightarrow}{\partial}_\mu \psi = \varphi \partial_\mu \psi - \psi \partial_\mu \varphi.$$

Contribution of the third term in the right hand side of Eq. (13) is zero identically. Indeed, using Eq. (12), and performing spacetime integrations we see that the three lines coming, say, into z -vertex are all on the mass shell, which is inconsistent with the momentum conservation in the vertex. Taking the Fourier transform of $I_{\mu\nu}(x, x')$,

$$\tilde{I}_{\mu\nu}(\mathbf{x}, \mathbf{x}', t', \omega) = \int_{-\infty}^{+\infty} dt I_{\mu\nu}(x, x') e^{i\omega(t-t')},$$

the remaining terms in Eq. (13) take the form

$$\begin{aligned} \tilde{I}_{\mu\nu}(\mathbf{x}, \mathbf{x}', t', \omega) &= e^2 \iint \frac{d^3\mathbf{q}}{(2\pi)^3} \frac{d^3\mathbf{p}}{(2\pi)^3} \frac{a^*(\mathbf{q})a(\mathbf{q}+\mathbf{p})}{\sqrt{2\varepsilon_{\mathbf{q}}2\varepsilon_{\mathbf{q}+\mathbf{p}}}} e^{-ip^0(t'-t_0)+i\mathbf{p}\mathbf{x}'} \tilde{J}_{\mu\nu}(p, q, \mathbf{x} - \mathbf{x}', \omega), \\ p^0 &= \varepsilon_{\mathbf{q}+\mathbf{p}} - \varepsilon_{\mathbf{q}}, \end{aligned} \quad (14)$$

where

$$\begin{aligned} \tilde{J}_{\mu\nu}(p, q, \mathbf{x} - \mathbf{x}', \omega) &= -i \int \frac{d^3\mathbf{k}}{(2\pi)^3} e^{i\mathbf{k}(\mathbf{x}-\mathbf{x}')} (2q_\mu + k_\mu)(2q_\nu + k_\nu + p_\nu) \\ &\times \left\{ D_{++}^0(k) D_{++}(q+k) D_{+-}^0(k-p) - D_{++}^0(k) D_{+-}(q+k) D_{--}^0(k-p) \right. \\ &\left. + D_{+-}^0(k) D_{--}(q+k) D_{--}^0(k-p) \right\}_{k^0=\omega}. \end{aligned} \quad (15)$$

Here $\varepsilon_{\mathbf{q}} = \sqrt{\mathbf{q}^2 + m^2}$ is the particle's energy, m , e , q_μ , and $a(\mathbf{q})$ are its mass, electric charge, 4-momentum, and momentum wave function at some time instant t_0 , p_μ 4-momentum transfer. The function $a(\mathbf{q})$ is normalized by

$$\int \frac{d^3\mathbf{q}}{(2\pi)^3} |a(\mathbf{q})|^2 = 1, \quad (16)$$

and is generally of the form

$$a(\mathbf{q}) = b(\mathbf{q}) e^{-i\mathbf{q}\mathbf{x}_0}, \quad (17)$$

where \mathbf{x}_0 is the particle mean position, and $b(\mathbf{q})$ describes the momentum space profile of the particle wave packet. For simplicity, the particle charge distribution will be assumed spherically-symmetric in what follows. Then $b(\mathbf{q})$ is a function of \mathbf{q}^2 : $b(\mathbf{q}) = \beta(\mathbf{q}^2)$.

As in Ref. [9], we work within the long-range expansion which implies, in particular, that the spatial separations between the field-producing particle (more precisely, its mean position) and the points of observation, $r = |\mathbf{x} - \mathbf{x}_0|$, $r' = |\mathbf{x}' - \mathbf{x}_0|$, are such that $r\bar{q} \gg 1$, $r'\bar{q} \gg 1$, where $\bar{q} = \sqrt{\langle \mathbf{q}^2 \rangle}$ is the particle momentum variance (note that \bar{q} is time-independent for a free particle). To the leading order of the long-range expansion, p_μ , k_μ in the vertex factors in Eq. (15) can be neglected in comparison with q_μ .

Let us now show that the low-frequency asymptotic of $\tilde{J}_{\mu\nu}$ is weaker than $1/\omega$. The first and the third terms in the integrand in Eq. (15) give rise to a contribution which is finite at $\omega = 0$. We have for the third term

$$\begin{aligned} & \int d^3\mathbf{k} e^{i\mathbf{k}(\mathbf{x}-\mathbf{x}')} D_{+-}^0(k) D_{--}(q+k) D_{--}^0(k-p) \Big|_{k^0=0} \\ &= \int d^2o \int_0^\infty d|\mathbf{k}| \frac{\mathbf{k}^2 e^{i\mathbf{k}(\mathbf{x}-\mathbf{x}')} 2\pi i \delta(\mathbf{k}^2)}{[-2(\mathbf{q}\mathbf{k}) - i0][p^2 + 2(\mathbf{p}\mathbf{k}) - i0]} = -\frac{\pi i}{4|\mathbf{q}|p^2} \int \frac{d\phi d\theta \sin\theta}{\cos\theta + i0} = -\frac{\pi^3}{2|\mathbf{q}|p^2}. \end{aligned}$$

Similarly,

$$\begin{aligned} & \int d^3\mathbf{k} e^{i\mathbf{k}(\mathbf{x}-\mathbf{x}')} D_{++}^0(k) D_{++}(q+k) D_{+-}^0(k-p) \Big|_{k^0=0} \\ &= \int d^2o \int_0^\infty d|\mathbf{k}| \frac{\mathbf{k}^2 e^{i\mathbf{k}(\mathbf{x}-\mathbf{x}')} 2\pi i \theta(p^0) \delta((p^0)^2 - (\mathbf{k} - \mathbf{p})^2)}{[\mathbf{k}^2 - i0][\mathbf{k}^2 + 2(\mathbf{q}\mathbf{k}) - i0]} \end{aligned}$$

is also finite for all \mathbf{p} and $\mathbf{q} \neq 0$ [the singularity at $\mathbf{q} = 0$ or $\mathbf{p} = 0$ in these expressions is inessential as it is removed by the factors \mathbf{q}^2 and \mathbf{p}^2 in the integral measure in Eq. (14)]. The second term in the integrand, however, leads to a divergence at $\omega = 0$. This divergence comes from integration over small $|\mathbf{k}|$. Hence, it is the same as the divergence of the integral

$$\int d^2o \int_0^\infty d|\mathbf{k}| \frac{\mathbf{k}^2 \delta(\omega^2 + 2m\omega - \mathbf{k}^2 - 2(\mathbf{q}\mathbf{k}))}{[-\omega^2 + \mathbf{k}^2 - i0][p^2 - i0]} = \frac{\pi}{|\mathbf{q}|p^2} \int_{\sqrt{\mathbf{q}^2 + \omega^2 + 2m\omega} - |\mathbf{q}|}^{\sqrt{\mathbf{q}^2 + \omega^2 + 2m\omega} + |\mathbf{q}|} \frac{udu}{-\omega^2 + u^2 - i0}.$$

The latter integral diverges for $\omega \rightarrow 0$ only logarithmically.

B. Low-frequency asymptotic of the disconnected part of correlation function

Let us turn to the disconnected part of the correlation function. To find its Fourier transform, we have to evaluate the following integral

$$\int_{-\infty}^{+\infty} dt \langle \text{in} | A_\mu(x) | \text{in} \rangle e^{i\omega(t-t')} = q_\mu e^{-i\omega t'} \tilde{I}(\mathbf{r}, \omega), \quad (18)$$

where

$$\tilde{I}(\mathbf{r}, \omega) = \int_{-\infty}^{+\infty} dt \left\{ e^{i\omega t} \iint \frac{d^3\mathbf{q}}{(2\pi)^3} \frac{d^3\mathbf{p}}{(2\pi)^3} \frac{e^{i\mathbf{p}\mathbf{r}}}{\mathbf{p}^2} e^{-ip^0(t-t_0)} b^*(\mathbf{q}) b(\mathbf{q} + \mathbf{p}) \right\}, \quad \mathbf{r} = \mathbf{x} - \mathbf{x}_0.$$

Substituting

$$p^0 \approx \frac{(\mathbf{p} + \mathbf{q})^2}{2m} - \frac{\mathbf{q}^2}{2m}$$

gives

$$\tilde{I}(\mathbf{r}, \omega) = 2\pi e^{i\omega t_0} \iint \frac{d^3\mathbf{q}}{(2\pi)^3} \frac{d^3\mathbf{p}}{(2\pi)^3} \delta\left(\omega - \frac{\mathbf{p}^2 + 2\mathbf{p}\mathbf{q}}{2m}\right) \frac{e^{i\mathbf{p}\mathbf{r}}}{\mathbf{p}^2} b^*(\mathbf{q}) b(\mathbf{q} + \mathbf{p}).$$

For a spherically-symmetric charge distribution, $b(\mathbf{q}) = \beta(q^2)$, \tilde{I} is actually a function of $r = |\mathbf{r}|$, $\tilde{I}(\mathbf{r}, \omega) = \tilde{I}(r, \omega)$, and hence, averaging over directions of \mathbf{r} , one can write

$$\begin{aligned} \tilde{I}(r, \omega) &= 2\pi e^{i\omega t_0} \iint \frac{d^3\mathbf{q}}{(2\pi)^3} \frac{d^3\mathbf{p}}{(2\pi)^3} \delta\left(\omega - \frac{\mathbf{p}^2 + 2\mathbf{p}\mathbf{q}}{2m}\right) \frac{\sin(pr)}{p^3 r} \beta^*(q^2) \beta(q^2 + 2m\omega) \\ &= \frac{m e^{i\omega t_0}}{2\pi r} \int \frac{d^3\mathbf{q}}{(2\pi)^3} \beta^*(q^2) \beta(q^2 + 2m\omega) \int_0^\pi d\theta \frac{\sin\theta \sin(ur)}{u \sqrt{q^2 \cos^2\theta + 2m\omega}}, \\ u &= -|\mathbf{q}| \cos\theta + \sqrt{q^2 \cos^2\theta + 2m\omega}, \end{aligned} \quad (19)$$

where θ is the angle between the vectors \mathbf{p}, \mathbf{q} , and it is assumed that $\omega > 0$. Taking u as the integration variable yields

$$\tilde{I}(r, \omega) = \frac{me^{i\omega t_0}}{8\pi^3 r} \int_0^{+\infty} d\mathbf{q}^2 \beta^*(\mathbf{q}^2) \beta(\mathbf{q}^2 + 2m\omega) \int_{\sqrt{\mathbf{q}^2 + 2m\omega} - |\mathbf{q}|}^{\sqrt{\mathbf{q}^2 + 2m\omega} + |\mathbf{q}|} du \frac{\sin(ur)}{u^2}. \quad (20)$$

To further transform this integral, it is convenient to define a function $\Gamma(\mathbf{q}^2, \omega)$ according to

$$\Gamma(\mathbf{q}^2, \omega) = \frac{1}{4\pi^2} \int_{\mathbf{q}^2}^{+\infty} dz \beta^*(z) \beta(z + 2m\omega). \quad (21)$$

Then integrating by parts, and taking into account that $\Gamma(\mathbf{q}^2, \omega) \rightarrow 0$ for $\mathbf{q}^2 \rightarrow \infty$, brings Eq. (20) to the form

$$\begin{aligned} \tilde{I}(r, \omega) = & \frac{me^{i\omega t_0}}{2\pi r} \int_0^{+\infty} d|\mathbf{q}| \frac{\Gamma(\mathbf{q}^2, \omega)}{\sqrt{\mathbf{q}^2 + 2m\omega}} \left\{ \frac{\sin(ur)}{u} \Big|_{u=\sqrt{\mathbf{q}^2 + 2m\omega} + |\mathbf{q}|} \right. \\ & \left. + \frac{\sin(ur)}{u} \Big|_{u=\sqrt{\mathbf{q}^2 + 2m\omega} - |\mathbf{q}|} \right\}. \end{aligned} \quad (22)$$

Finally, integrating \tilde{I} by parts once more, we find

$$\tilde{I}(r, \omega) = \frac{e^{i\omega t_0}}{2\pi r \omega} \int_0^{+\infty} d|\mathbf{q}| \sin\left(r\sqrt{\mathbf{q}^2 + 2m\omega}\right) \left\{ 2\Gamma \cos(|\mathbf{q}|r) + \frac{1}{r} \frac{\partial \Gamma}{\partial |\mathbf{q}|} \sin(|\mathbf{q}|r) \right\}. \quad (23)$$

This exact expression considerably simplifies in the practically important case of low ω and large r . Namely, if ω is such that

$$\omega \ll \frac{\bar{q}}{mr} \equiv \omega_0, \quad (24)$$

and also

$$r\bar{q} \gg 1$$

(and therefore, $\omega \ll \bar{q}^2/m$), then the first term in \tilde{I} turns out to be exponentially small ($\sim e^{-r\bar{q}}$) because of the oscillating product of trigonometric functions. Replacing $\sin^2(qr)$ by its average value $(1/2)$ in the rest of \tilde{I} gives

$$\tilde{I}(r, \omega) = \frac{e^{i\omega t_0}}{4\pi r^2 \omega} \int_0^{+\infty} d|\mathbf{q}| \frac{\partial \Gamma}{\partial |\mathbf{q}|} = -\frac{e^{i\omega t_0} \Gamma(0, 0)}{4\pi r^2 \omega} = -\frac{e^{i\omega t_0}}{16\pi^3 r^2 \omega} \int_0^{+\infty} dz |\beta(z)|^2. \quad (25)$$

Substituting the obtained expression into the defining equations (18), (10), (11), we thus obtain the following expression for the low-frequency asymptotic of the correlation function

$$C_{00}(\mathbf{x}, \mathbf{x}', t', \omega) = e^{i\omega(t_0 - t')} \frac{e^2}{16\pi^3 r^2 \omega} \int_0^{+\infty} dz |\beta(z)|^2 \iint \frac{d^3 \mathbf{q}}{(2\pi)^3} \frac{d^3 \mathbf{p}}{(2\pi)^3} \frac{e^{-ip(\mathbf{x}' - \mathbf{x}_0)}}{\mathbf{p}^2} \beta^*(\mathbf{q}^2) \beta((\mathbf{q} + \mathbf{p})^2), \quad (26)$$

all other components of $C_{\mu\nu}$ being suppressed by the factor $|\mathbf{q}|/m \ll 1$. For the time instants t' such that $r, r' \gg D_{t'}$, where $D_{t'}$ is a characteristic linear dimension of the particle charge distribution (for instance, variance of the particle coordinates), Eq. (26) simplifies to

$$C_{00}(\mathbf{x}, \mathbf{x}', t', \omega) = e^{i\omega(t_0 - t')} \frac{e^2}{64\pi^4 r^2 r' \omega} \int_0^{+\infty} dz |\beta(z)|^2. \quad (27)$$

In applications to microelectronics, ω varies from 10^{-6} Hz to 10^6 Hz, the relevant distances r are usually 10^{-5} cm to 10^{-2} cm, $\bar{q} \sim \hbar/d$, where $d \approx 10^{-8}$ cm is the lattice spacing, and m is the effective electron mass, $m \approx 10^{-27}$ g, hence, $\omega_0 \approx 10^{10}$ Hz, so the conditions $r \gg d$, $\omega \ll \omega_0$ are always well-satisfied.

Equation (27) represents an individual contribution of a conduction electron to the electric potential fluctuation. Considering a large number of uncorrelated electrons in a sample, one should take into account that the corresponding time instants t_0 are distributed uniformly. Because of the oscillating exponent $e^{i\omega(t_0-t')}$, the magnitude of the total noise remains at the level of the individual contribution independently of the number of electrons. Therefore, summing up all contributions amounts simply to averaging over \mathbf{x}_0 :

$$|C_{00}^{\text{tot}}(\mathbf{x}, \mathbf{x}', \omega)| = \frac{e^2}{64\pi^4|\omega|\Omega} \int_0^{+\infty} dz |\beta(z)|^2 \int_{\Omega} \frac{d^3\mathbf{x}_0}{r^2 r'}, \quad (28)$$

where Ω is the sample volume. To visualize it, one can say that various uncompensated individual contributions “flicker” in various points of the sample.

It is clear from the above discussion that the distribution of the noise magnitude around the value C_{00}^{tot} is Gaussian, by virtue of the central limiting theorem. Thus, the quantum field fluctuations in a sample possess the above-mentioned property 2).

Next, let us consider the case when the sample is in an external electric field, \mathbf{E} . Under the influence of the external field, both the electron wave functions and the statistical probability distribution are changed. It turns out, however, that in practice, the change of the wave functions is negligible. Namely, a direct calculation shows that the relative value of the correction is of the order

$$\kappa_q = \frac{\hbar^2 m e |\mathbf{E}|}{\bar{q}^4 L},$$

where L is the smallest linear dimension of the sample. Using the above estimates for \bar{q} , L in the condition $\kappa_q \ll 1$ gives $|\mathbf{E}| \ll 10^{10}$, in the *cgs* system of units. In applications to microelectronics, the field strength is usually $|\mathbf{E}| \lesssim 1$, so $\kappa_q \approx 10^{-10}$. On the other hand, the relative change of the statistical distribution function, given by the kinetic theory, is of the order

$$\kappa_s = \frac{e |\mathbf{E}| l}{\bar{\varepsilon}},$$

where l is the electron mean free path, and $\bar{\varepsilon}$ its mean energy, $\bar{\varepsilon} \approx \hbar^2/m d^2$. κ_s is generally not small. Furthermore, the statistical distribution is generally analytic in \mathbf{E} in a vicinity of $\mathbf{E} = 0$, and hence the leading correction to the scalar quantity C_{00} is proportional to \mathbf{E}^2 [property 3)].

Because of collisions with phonons and impurities in the crystal, evolution of the conduction electrons usually cannot be considered free. It is important, however, that in view of the smallness of the electron mass in comparison with the mass of the lattice atoms, these collisions may often be considered elastic. In such collisions, the electron energy is not changed, and therefore, so is time evolution of the electron wave function. Hence, the above results concerning dispersion of the electromagnetic field fluctuations remain essentially the same upon account of the electron collisions, except that now they must be expressed in terms of the electron density matrix, rather than wave function. Denoting the momentum space density matrix of the electron by $\rho(\mathbf{p}^2, \mathbf{q}^2)$, Eq. (28) thus takes the form

$$|C_{00}^{\text{tot}}(\mathbf{x}, \mathbf{x}', \omega)| = \frac{e^2 \Gamma_0}{16\pi^2 |\omega| \Omega} \int_{\Omega} \frac{d^3\mathbf{x}_0}{r^2 r'}, \quad \Gamma_0 \equiv \frac{1}{4\pi^2} \int_0^{+\infty} dz \rho(z, z). \quad (29)$$

The quantity denoted here by Γ_0 is nothing but the expectation value of the inverse particle momentum:

$$\Gamma_0 = \int \frac{d^3\mathbf{q}}{(2\pi)^3} \frac{\rho(\mathbf{q}^2, \mathbf{q}^2)}{|\mathbf{q}|} = \left\langle \frac{1}{|\mathbf{q}|} \right\rangle.$$

Hence, by the order of magnitude, $\Gamma_0 \approx 1/\bar{q}$ (in the ordinary units, $\Gamma_0 \approx \hbar/\bar{q}$.)

In practice, one is interested in fluctuations of the voltage, U , between two leads attached to a sample. Using the above results, it is not difficult to write down an expression for the voltage correlation function, $C_U(\mathbf{x}, \mathbf{x}', \omega)$. We have

$$\begin{aligned} \langle \text{in} | U(\mathbf{x}, \mathbf{x}', t) | \text{in} \rangle \langle \text{in} | U(\mathbf{x}, \mathbf{x}', t') | \text{in} \rangle &= \langle \text{in} | A_0(\mathbf{x}, t) - A_0(\mathbf{x}', t) | \text{in} \rangle \langle \text{in} | A_0(\mathbf{x}, t') - A_0(\mathbf{x}', t') | \text{in} \rangle \\ &= \langle \text{in} | A_0(\mathbf{x}, t) | \text{in} \rangle \langle \text{in} | A_0(\mathbf{x}, t') | \text{in} \rangle + \langle \text{in} | A_0(\mathbf{x}', t) | \text{in} \rangle \langle \text{in} | A_0(\mathbf{x}', t') | \text{in} \rangle \\ &\quad - \langle \text{in} | A_0(\mathbf{x}', t) | \text{in} \rangle \langle \text{in} | A_0(\mathbf{x}, t') | \text{in} \rangle - \langle \text{in} | A_0(\mathbf{x}, t) | \text{in} \rangle \langle \text{in} | A_0(\mathbf{x}', t') | \text{in} \rangle. \end{aligned} \quad (30)$$

Fourier transforming and applying Eq. (27) to each of the four terms in this expression, we obtain the low-frequency asymptotic of the overall voltage fluctuation across the sample

$$|C_U^{\text{tot}}(\mathbf{x}, \mathbf{x}', \omega)| = \frac{e^2 \Gamma_0 G}{16\pi^2 |\omega| \Omega}, \quad (31)$$

where

$$G \equiv \int_{\Omega} d^3 \mathbf{x}_0 \left(\frac{1}{r^3} + \frac{1}{r'^3} - \frac{1}{r^2 r'} - \frac{1}{r'^2 r} \right). \quad (32)$$

Let us discuss the role of the sample geometry in somewhat more detail. Consider two geometrically similar samples, and let n be the ratio of their linear dimensions (see Fig. 3). Such samples are characterized by the same value of the G -factor. Indeed, the voltage across each sample is measured via two leads attached to its surface. Hence, the radius-vectors of the leads drawn from the center of similitude scale by the same factor n , and therefore,

$$\begin{aligned} \int_{\Omega_2} \frac{d^3 \mathbf{x}_0}{r^2 r'} &= \int_{n^3 \Omega_1} \frac{d^3 \mathbf{x}_0}{|n\mathbf{x} - \mathbf{x}_0|^2 |n\mathbf{x}' - \mathbf{x}_0|} = \int_{\Omega_1} \frac{n^3 d^3(\mathbf{x}_0)}{|n\mathbf{x} - n\mathbf{x}_0|^2 |n\mathbf{x}' - n\mathbf{x}_0|} \\ &= \int_{\Omega_1} \frac{d^3 \mathbf{x}_0}{|\mathbf{x} - \mathbf{x}_0|^2 |\mathbf{x}' - \mathbf{x}_0|} = \int_{\Omega_1} \frac{d^3 \mathbf{x}_0}{r^2 r'}, \end{aligned}$$

and likewise for the other terms in Eq. (32). Thus, it follows from Eq. (28) that for geometrically similar samples, the noise level is inversely proportional to the sample volume [property 1)].

It is worth also to make the following comment concerning Eq. (32). The integrand in this formula involves the terms $1/r^3$ and $1/r'^3$ which give rise formally to a logarithmic divergence when the observation points approach the sample. In this connection, it should be recalled that the above calculations have been carried out under the condition $r\bar{q} \gg 1$, hence, r, r' cannot be taken too small. Furthermore, one should remember that in any field measurement in a given point, one deals actually with the field averaged over a small but finite domain surrounding this point, i.e., the voltage lead in our case. Thus, for instance, the quantity $A_0(\mathbf{x}, t)$ appearing in the expression (30) is to be substituted by

$$\mathcal{A}_0 = \frac{1}{\Omega_L} \int_{\Omega_L} d^3 \mathbf{x} A_0(\mathbf{x}, t),$$

where Ω_L is the voltage lead volume. As the result of this substitution, the term $1/r^3$ takes the form

$$\frac{1}{\Omega_L^2} \iint_{\Omega_L} \frac{d^3 \mathbf{x} d^3 \tilde{\mathbf{x}}}{|\mathbf{x} - \mathbf{x}_0|^2 |\tilde{\mathbf{x}} - \mathbf{x}_0|}.$$

This is finite however the lead is attached to the sample. Equation (32) is recovered in the case when r, r' are much larger than the sample size.

C. A preliminary comparison with experiment

For a preliminary comparison of the noise level given by Eq. (31) with experimental data, let us use the results of the classic paper by Voss and Clarke [5] where the $1/f$ -noise in continuous Bi and Au films was measured. The bismuth and gold samples had dimensions $1000 \text{ \AA} \times 10 \mu\text{m} \times 120 \mu\text{m}$ and $250 \text{ \AA} \times 8 \mu\text{m} \times 625 \mu\text{m}$, respectively. The spectrum power for $f = \omega/2\pi = 1 \text{ Hz}$ and $|\mathbf{E}| = 0$ was found to be about $10^{-14} \text{ V}^2/\text{Hz}$ in the case of Bi sample, and about $10^{-16} \text{ V}^2/\text{Hz}$ in the case of Au sample (it is assumed here that the contributions from external pickup and amplifier noise in the experimental setup of Ref. [5] do not dominate over the sample noise component).

For a rough estimate of the right hand side of Eq. (31) we take $\Gamma_0 \approx \hbar/\bar{q} \approx d \approx 10^{-8} \text{ cm}$, and note that $\Omega \approx 10^{-10} \text{ cm}^3$ for both samples. However, the G -factor takes different values for the two sample configurations. It is seen from Eq. (32) that for elongated samples of fixed volume, G decreases roughly as the inverse sample length. Evaluating the G -factor as explained in the preceding section gives $G = 0.03$ for Bi sample, and $G = 0.007$ for Au sample. Substitution of the above estimates into Eq. (31) gives the order of magnitude of the noise spectrum power $10^{-15} \text{ V}^2/\text{Hz}$, and $10^{-16} \text{ V}^2/\text{Hz}$ for Bi and Au sample, respectively. We see that in both cases the theoretical estimates are in a reasonable agreement with the experimental data. A more detailed comparison is a much more difficult task which would require specification of the precise form of the function $\beta(z)$.

IV. CONCLUSIONS

We have shown that in the whole measured frequency band, the power spectrum of quantum fluctuations of the Coulomb field exhibits an inverse frequency dependence [Cf. Eq. (31)]. This result is obtained by evaluating the two-point correlation function of the electromagnetic field within the long-range expansion. It was proved, in particular, that the low-frequency asymptotic of the Fourier transform of this function is dominated by its disconnected part. Furthermore, we have argued that the derived power spectrum possesses the other experimentally observed properties of the $1/f$ -noise as well. In particular, the exact dependence of flicker noise on the sample geometry has been established. That the power spectrum of flicker noise is proportional to the sample volume only very approximately was noticed long ago, but precise form of this dependence has not been inferred. We have shown that for geometrically similar samples the noise power spectrum is inversely proportional to the sample volume, while for samples of the same volume dependence on the sample geometry is described by the dimensionless G -factor given by Eq. (32).

Finally, according to the semi-quantitative estimates of Sec. III C, the found noise level is in a reasonable agreement with experimental data. Thus, quantum fluctuations of the Coulomb field produced by elementary particles can be considered as one of the underlying mechanisms of the observed $1/f$ -noise.

Acknowledgments

I thank Drs. G. A. Sardanashvili, K. V. Stepanyantz (Moscow State University) for interesting discussions, and especially P. I. Pronin for introducing me into the problem of $1/f$ -noise.

-
- [1] M. Buckingham, *Noise in Electronic Devices and Systems* (Chichester: Ellis Horwood, 1983).
 - [2] F. N. Hooge, *Physica (Utr.)* **60**, 130 (1972).
 - [3] Th. G. M. Kleinpenning, *Physica (Utr.)* **77**, 78 (1974).
 - [4] A. L. McWhorter, *Semiconductor Surface Physics*, edited by R. H. Kingston (University of Pennsylvania, Philadelphia, 1957), p. 207.
 - [5] R. F. Voss and J. Clarke, *Phys. Rev. B* **13**, 556 (1976).
 - [6] P. H. Handel, *Phys. Rev. Lett.* **34**, 1492 (1975); *Phys. Rev. A* **22**, 745 (1980); a fairly complete bibliography on the quantum theory approach to the $1/f$ -noise can be found at <http://www.umsi.edu/~handel/QuantumBib.html>
 - [7] A.-M. Tremblay, thesis, Massachusetts Institute of Technology, 1978.
 - [8] Th. M. Nieuwenhuizen, D. Frenkel and N. G. van Kampen, *Phys. Rev. A* **35**, 2750 (1987).
 - [9] K. A. Kazakov, *Phys. Rev. D* **71**, 113012 (2005).
 - [10] J. Schwinger, *J. Math. Phys.* **2**, 407 (1961); *Particles, Sources and Fields* (Addison-Wesley, Reading, Mass., 1970).
 - [11] L. V. Keldysh, *Zh. Eksp. Teor. Fiz.* **47**, 1515 (1964) [*Sov. Phys. JETP* **20**, 1018 (1965)].

Figure captions

Fig.1: Tree contribution to the right hand side of Eq. (2). Wavy lines represent photon propagators, solid lines the scalar particle.

Fig.2: Tree contribution to the right hand side of Eq. (9). Part (e) of the figure represents the “transposition” of diagrams (a)–(d) (see Sec. IIIB).

Fig.3: Voltage measurement in geometrically similar samples ($n = 2$).

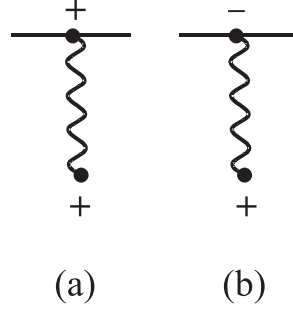


FIG. 1:

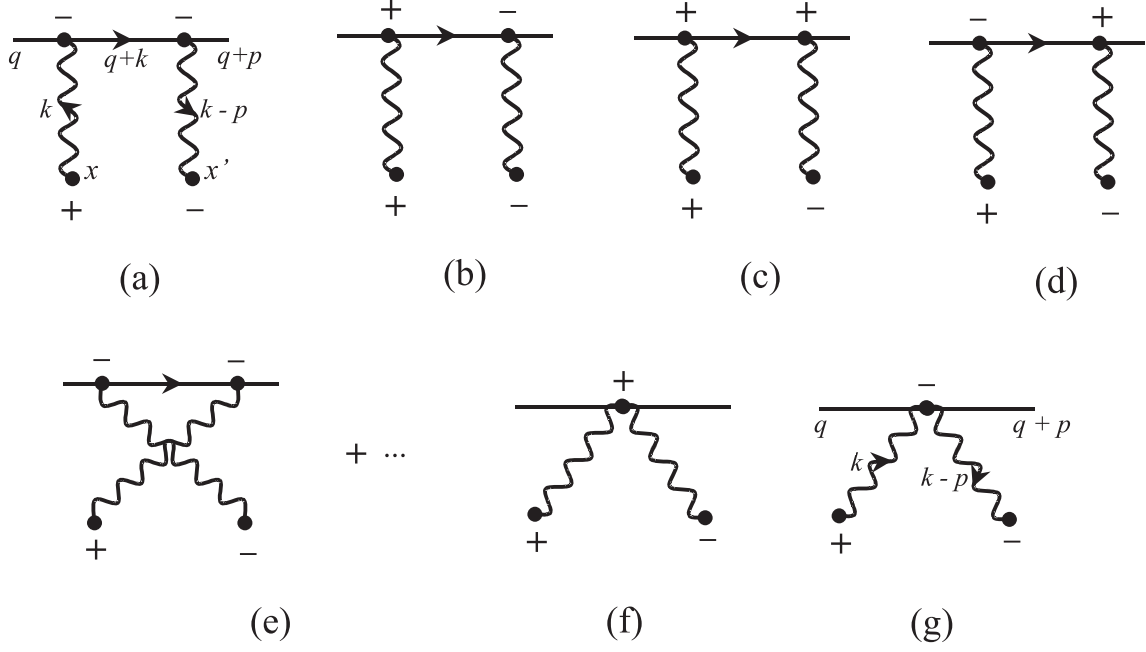


FIG. 2:

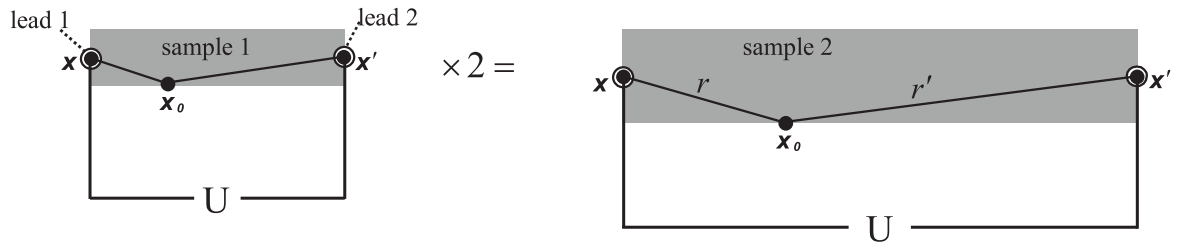


FIG. 3: